Double photoionization of neon*

T. N. Chang†
Department of Physics, University of Chicago, Chicago, Illinois 60637

R. T. Poe
Department of Physics, University of California, Riverside, California 92502

(Received 10 April 1975)

A calculation of the double photoionization of neon using many-body perturbation theory has permitted a quantitative study of the relative importance of various contributing effects, i.e., ground-state correlations, inelastic internal collisions, core rearrangement, and a virtual Auger transition. The results are in good agreement with experimental data. The energy distribution between two outgoing electrons and the ratio of double to single photoionization are calculated and discussed.

I. INTRODUCTION

Multiple photoionization has been one of the major unsolved problems in atomic and molecular photoabsorption processes.[1,2] Extensive experimental investigations on the multiple photoionization of rare-gas atoms have been carried out in recent years.[3-9] On the higher-energy side, where the photon energy is sufficiently high to ionize an inner-shell electron, the dominant contributing mechanism is the Auger transition. Another important physical process which contributes significantly at this energy range, commonly known as the "shake-off" process, has been adequately understood through the use of the sudden approximation.[2-4] Agreement between experimental observation and theoretical estimation is in general satisfactory. On the other hand, in the lower-energy region, where both electrons originate from the same valence shell, the observed double-photoionization intensity has been known to be in large excess over the predictions of the single-particle sudden approximation.[3] This has led to a large number of experimental investigations with various independent approaches in the past few years.[5-9] Although considerable discrepancies exist among various experimental measurements, all the experimental evidence tends to suggest that any satisfactory physical interpretation of the multiple photoionization process would require more detailed understanding of various many-particle interactions.

While extensive experimental data on multiple photoionization are available, detailed theoretical investigations including many-particle effects have been carried out only in a few cases. A calculation with extensive ground-state configuration mixing and with an uncorrelated final-state Coulomb wave function by Byron and Joachain[10] has accounted for the observed double photoionization of helium in a wide range of energy (about 100–500 eV). However, the extension of this treatment to other heavier atoms, where other complicated many-particle effects may be important, is by no means obvious. The only other detailed theoretical calculation has been an investigation of Ne double photoionization at $h\nu = 278$ eV by a many-body perturbation-theory (MBPT) approach.[11] This study has shown that several physical effects, namely, ground-state electron-electron correlations, core rearrangement, and a virtual Auger transition, must be considered together to obtain good agreement with the results of Carlson's experiment, both with regard to the photoelectron energy spectrum and to the ratio of double to single photoionization cross sections. The major advantage of this approach, aside from its ability to incorporate various many-particle interactions into one general formalism, has been the possibility of identifying each contributing physical effect with its corresponding term in the perturbation expansion, leading to a more transparent physical interpretation of the multiple photoionization process. However, a large discrepancy between experimental data in that energy region (~200 eV) has prevented this theoretical treatment from being established as an acceptable approach without any further assessment.[12]

This paper reports the result of a more extensive calculation, based on the MBPT approach, of double photoionization of Ne throughout the energy range from threshold to about 220-eV photon energy. The main emphasis is on a quantitative estimation of the relative importance of various contributing effects in different energy regions. The results of the present calculation are compared with available experimental data, and the discussion will cover various physical aspects and their implications for multiple photoionization.

II. PHYSICAL CONSIDERATIONS AND MBPT APPROACH

We limit our present discussion to double electron ejection from the outermost shell of rare-gas

atoms, regarding it as a first step in a systematic study. More specifically, we consider the process

$$A(1s^2 2s^2 \cdots ns^2 np^6) + \hbar\omega \rightarrow A^{++}(1s^2 2s^2 \cdots ns^2 np^4) + e^-(k_1 p) + e^-(k_2 d), \tag{2.1}$$

where k_i are the momenta of ejected electrons. The energy-conservation relation for this process is given in atomic units by

$$\tfrac{1}{2}k_1^2 + \tfrac{1}{2}k_2^2 + E_{A^{++}} = E_\gamma + E_A, \tag{2.2}$$

where E_γ is the photon energy, and E_A and $E_{A^{++}}$ are the total energies of the neutral atom A and residual ion A^{++}, respectively. (In the present calculation, the energy $E_{A^{++}}$ is given by the average value over three ionic states ^3P, ^1S, and ^1D.)

A. Physical considerations

As we pointed out in Sec. I, three physical effects—core rearrangement, ground-state correlations, and a virtual Auger transition—contribute significantly to the double photoionization of Ne in the soft-x-ray region. We now discuss briefly these effects and other processes which may also contribute significantly in other energy ranges.

i. Core rearrangement. An electron being ionized by photoabsorption ceases to contribute to the screening of the nuclear charge. This change in the screening is experienced by the rest of the electrons, and their resultant rearrangement may lead to the simultaneous removal of one of them. This phenomenon, commonly referred to as "shake-off" process, is the main mechanism responsible for double photoionization when the two ejected electrons come from different shells. Although this process *alone* fails to describe double photoionization adequately when both ejected electrons come from the valence shell, it remains one of the important contributing effects.

ii. Ground-state correlations. Both experimental and theoretical investigations have indicated that electron-electron correlations in the ground state play an important part in double photoionization. This is particularly evident in the calculation by Byron and Joachain, where a correlated ground-state wave function is used to give a correct account of the helium double photoionization.

iii. Virtual Auger transition. This process involves three orbital electrons. Photoionization of an *ns* electron is followed by an Auger process involving two *np* electrons, one of which drops to the *ns* orbit while the other is ionized. This process is termed "virtual" because energy is not conserved in its intermediate state.

iv. Inelastic internal collision. Direct collisions between a fast outgoing primary photoelectron and the other *np* electrons are negligible at higher energy. At lower energy, however, this process is expected to become more important, since the less energetic outgoing electron is more likely to exchange energy, momentum, and angular momentum with other *np* electrons, leading to the removal of a second electron.

The present calculation does not include other physical effects involving (a) transition to states other than p or d, (b) more than two orbital electrons, and (c) interactions between electrons of different shells (different n orbitals), although they may be important under different circumstances (especially for heavier atoms). We will discuss their significance in Sec. III.

B. MBPT approach

In this section, we briefly summarize some important elements of the MBPT approach[13,14] and its application to the double photoionization process. In this approach the Hamiltonian H of an N-electron atomic system in the presence of an external field H_γ is given by

$$H = H_0 + H', \tag{2.3}$$

where

$$H_0 = \sum_{i=1}^{N} (T_i + V_i), \tag{2.4}$$

$$H' = H_\gamma + \sum_{i<j}^{N} \frac{e^2}{r_{ij}} - \sum_{i=1}^{N} V_i. \tag{2.5}$$

The single-particle operator T_i represents the sum of the kinetic-energy operator and the nuclear potential of the ith electron. The single-particle potential V_i is chosen to represent an appropriate average for the system of interest. Eigenstates Φ_n of the unperturbed atomic system, given by $H_0\Phi_n = E_n\Phi_n$, can be expressed as combinations of Slater determinants of a complete set of single-particle orbitals φ_n, each of which satisfies the equation

$$(T + V)\varphi_n = \epsilon_n \varphi_n. \tag{2.6}$$

The ground state Φ_0 contains N orbitals which are lowest in energy.

To treat double photoionization, we have chosen a single-particle potential of the V^{N-1} type[13] which yields unexcited atomic orbitals identical to the Hartree-Fock self-consistent orbitals, while the excited single-particle orbitals are generated in the Hartree-Fock field of the neutral atom minus

one of the outer electrons. In the MBPT approach,[11,13-15] the lowest-order terms contributing to double photoionization are those quadratic in H' (but linear in H_γ). They are represented by the diagrams shown in Fig. 1, where a wavy line stands for the external field H_γ and horizontal dashed lines for the electron-electron interactions.

Diagram 1(a) represents the core rearrangement effect. This term results from the incomplete cancellation between two terms as shown in Fig. 2. The first term [diagram 2(a)] contains the interactions between one particle-hole pair (np_1, k_1p) and four other np electrons, while the second term [2(b)] represents the five interactions of this type included in our V^{N-1} potential; their combination reduces to a single term given by diagram 2(c) [or diagram 1(a)]. Diagram 1(b) represents ground-state correlations of np electrons. In the present calculations, we have included under the labels "k_0" and "$k_1 l_1$," the two most important configurations, $(np^4 n'p\, n''p)$ and $(np^4 n'd\, n''d)$, which lead to the same final-state configuration $(np^4 k_1 p\, k_2 d)$. Diagram 1(c) represents the virtual Auger transition involving one ns and two np electrons. Diagram 1(d) represents the direct collision between the primary outgoing electron and another np electron in the same atom, leading to the ionization of this second electron. Other processes, such as the ground-state correlations involving ns and np electrons, represented by diagram 1(e), are expected to be negligible.

With regard to higher-order terms, we have taken into account *semiempirically* the interactions between hole states, which are responsible for the energy corrections,[13] by using the experimentally determined energy-conservation relation, Eq. (2.2), instead of the relation

$$\tfrac{1}{2}k_1^2 + \tfrac{1}{2}k_2^2 = E_\gamma + 2\epsilon_{np} \tag{2.7}$$

that one would otherwise use if only the lowest-order term is considered. No other higher-order terms are included in our calculation.

As we mentioned before, the single-particle wave functions used in the present calculation are generated in a V^{N-1} type of potential field such that each of the outgoing electrons experiences asymptotically an attractive Coulomb potential due to a *single* charge. The radial part of the single-particle wave function $\varphi_{kl}(\vec{r})$ of each outgoing electron has the asymptotic form

$$R_{kl}(r) \underset{r\to\infty}{\longrightarrow} (1/r)\sin[kr + (1/k)\ln(2kr) - \tfrac{1}{2}l\pi + \delta_l], \tag{2.8}$$

where the potential in which $R_{kl}(r)$ is calculated is e^2/r as r approaches infinity. On the other hand, for double photoionization, each of the outgoing electrons should experience an attractive Coulomb force due to two charges at a large distance from the nucleus. Therefore, as r increases, the single-particle wave function generated in the V^{N-1} potential starts deviating from the correct asymptotic values. To minimize the error caused by this defect of the single-particle wave function, we have employed the dipole velocity approximation, which weights the wave function at small and intermediate distances more heavily.[16]

The total cross section for double photoionization in the dipole velocity approximation at a given photon energy E_γ is given by

$$\sigma_V(E_\gamma) = \frac{16\alpha a_0 e^2}{E_\gamma} \sum_f \int \frac{dk_1}{k_2} |T_f(k_1, k_2)|^2, \tag{2.9}$$

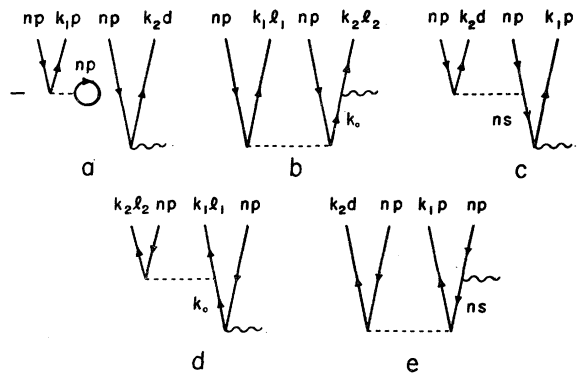

FIG. 1. Diagrams representing important contributing effects in double photoionization of rare-gas atoms. The wavy lines stand for photon interaction H_γ; dashed lines represent the electron-electron interaction.

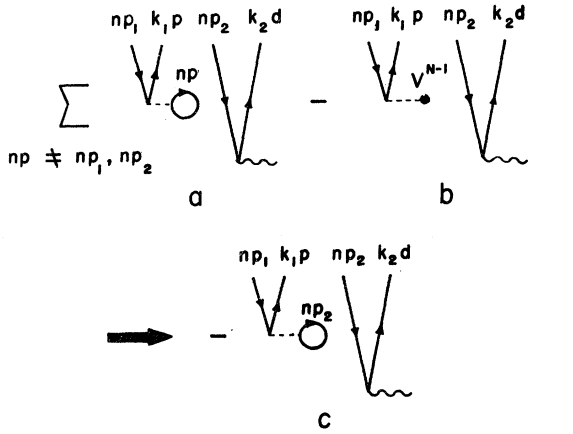

FIG. 2. Core-rearrangement-effect results from the incomplete cancellation of two lowest-order contributing terms.

where the summation is taken over all doubly ionized final states, and α and a_0 indicate the fine-structure constant and the Bohr radius, respectively. $T_f(k_1, k_2)$ is the sum of the matrix elements for all transitions to the same final state:

$$T_f(k_1, k_2) = \sum_\alpha t_\alpha^f(k_1, k_2) . \tag{2.10}$$

Table I gives the matrix-element expressions t_α^f of all contributing mechanisms shown in Fig. 1. The photoelectron energy spectrum for a given E_γ is represented by the cross section of a photoelectron at a particular pair of energies ϵ_1 and ϵ_2 (or k_1 and k_2):

$$\frac{d\sigma}{d\epsilon}(E_\gamma) = \sigma(k_1, k_2) + \sigma(k_2, k_1) , \tag{2.11}$$

where

$$\sigma(k_1, k_2) = \sum_f \frac{16\alpha a_0 e^2}{E_\gamma} \frac{1}{k_1 k_2} |T_f(k_1, k_2)|^2 . \tag{2.12}$$

Numerically, we first evaluate the matrix element $t_\alpha^f(k_1, k_2)$ at fixed k_1 and k_2 (each of them at nine predetermined values ranging from 0.1 to 4.5) for each contributing diagram α. This is done without reference to the photon energy E_γ. The matrix elements of diagrams 1(a), 1(c), and 1(e) can be readily evaluated for each pair of values of k_1 and k_2. For diagrams 1(b) and 1(d), the sum over a complete set of intermediate states k_0 is obtained by a differential-equation technique described elsewhere.[15,17]

TABLE I. Matrix element expressions t_α^f for all diagrams given in Fig. 1. [a]

Diagram (α)	Matrix element $[t_\alpha^f(k_1 k_2)]$
1(a)	$-\dfrac{\langle k_1 pnp \mid v \mid npnp\rangle \langle k_2 d \mid H_\gamma \mid np\rangle}{E_\gamma + \epsilon_{np} - \epsilon_{k_2}}$
1(b)	$\sum_{k_0} \dfrac{\langle k_2 l_2 \mid H_\gamma \mid k_0\rangle \langle k_0 k_1 l_1 \mid v \mid npnp\rangle}{2\epsilon_{np} - \epsilon_{k_1} - \epsilon_{k_0}}$
1(c)	$\dfrac{\langle k_2 dns \mid v \mid npnp\rangle \langle k_1 p \mid H_\gamma \mid ns\rangle}{E_\gamma + \epsilon_{ns} - \epsilon_{k_1}}$
1(d)	$\sum_{k_0} \dfrac{\langle k_2 l_2 k_1 l_1 \mid v \mid npk_0\rangle \langle k_0 \mid H_\gamma \mid np\rangle}{E_\gamma + \epsilon_{np} - \epsilon_{k_0}}$
1(e)	$\dfrac{\langle ns \mid H_\gamma \mid np\rangle \langle k_2 dk_1 p \mid v \mid npns\rangle}{\epsilon_{np} + \epsilon_{ns} - \epsilon_{k_1} - \epsilon_{k_2}}$

[a] $\langle ab \mid v \mid cd\rangle = \int\int d\vec{r}_1 d\vec{r}_2 \varphi_a^*(\vec{r}_1)\varphi_b^*(\vec{r}_2) \times (e^2/r_{12})\varphi_c(\vec{r}_1)\varphi_d(\vec{r}_2)$;

$\langle a \mid H_\gamma \mid b\rangle = \int d\vec{r}\, \varphi_a^*(\vec{r}) H_\gamma(\vec{r})\varphi_b(\vec{r})$.

In a second step, we obtain the matrix elements $t_\alpha^f(k_1, k_2)$ for each photon energy E_γ by selecting values of k_1 and k_2 in accordance with Eq. (2.2) and using Lagrange interpolation procedure. The dimension of the interpolated matrix t_α^f may be chosen appropriately for each photon energy. This procedure considerably reduced the computational effort.

III. RESULTS AND DISCUSSIONS

A. Oscillator strengths

Figure 3 gives our calculated oscillator strengths of Ne double photoionization for photon energies up to 220 eV. Curve A represents the contribution of the core-rearrangement effect [Fig. 1(a)] alone. Curve B results from the combined contribution of core rearrangement, ground-state correlations, and virtual Auger transitions [i.e., diagrams 1(a)–1(c)]. Although the individual contributions from the ground-state correlations or virtual Auger transition are smaller than that of core rearrangement, the combined contribution of these three effects is increased by more than two times at larger energies but decreased considerably on the lower-energy side. Curve C represents the combined oscillator strength arising from all final-state interactions, i.e., core rearrangement, virtual Auger transition, and inelastic internal collisions [diagrams 1(a), 1(c), and 1(d)]. Curve D gives the total oscillator

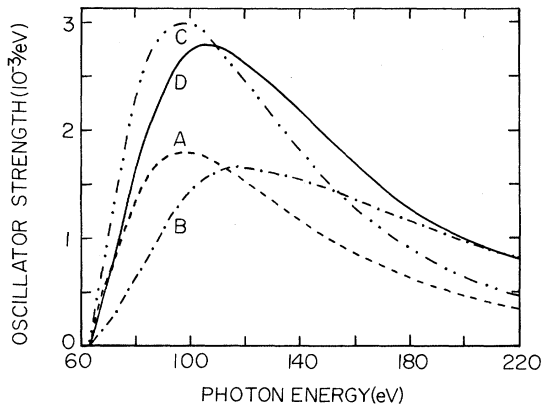

FIG. 3. Calculated oscillator strengths: curve A—core rearrangement [diagram 1(a)]; curve B—core rearrangement, ground-state correlations, and virtual Auger transition [diagrams 1(a) + 1(b) +1(c)]; curve C—core rearrangement, virtual Auger transition, and inelastic internal collision [diagrams 1(a) +1(c) +1(d)]; curve D—total contribution [diagrams 1(a) +1(b) +1(c) +1(d) +1(e)].

strength including all contributions shown in Fig. 1. The difference between curves B and D remains large up to about 170 eV, indicating that the effect of inelastic internal collision is still significant even at photon energies about 100 eV above the threshold. At even higher energies, curve B merges with curve D, indicating that the effect of inelastic internal collision becomes negligible.

B. Photoelectron energy spectrum

The total kinetic energy of the photoelectrons is given by $E = \frac{1}{2}k_1^2 + \frac{1}{2}k_2^2$. In Fig. 4, we present the photoelectron energy spectra for $E = 5$, 10, 20, 45, and 90 eV. Our calculation indicates that at higher energies, one of the outgoing electrons carries away most of the available energy, leaving very little energy to the other. This effect has been observed experimentally[3] and has also been derived theoretically in our previous calculation.[11] On the other hand, when the photon energy decreases, it becomes more likely for the two outgoing electrons to carry away comparable amounts of energy. This trend is consistent with the result derived both classically and quantum mechanically by Wannier and others[18] that each of the electrons has a constant probability to carry away any fraction of the available energy near the threshold for double ionization.

C. Comparison with experiments

Several experimental measurements on double photoionization of Ne from the outermost shell have been carried out over an extensive range of photon energies. Utilizing the techniques of charged-ion and photoelectron spectrometry, Carlson[3] has measured the relative abundances of doubly and singly charged ions as well as the photoelectron energy spectrum following x-ray absorption up to about 500 eV. From a high-energy electron-impact experiment, Van der Wiel and Wiebes[7] have extracted the oscillator strength of double ionization from threshold up to about 250 eV. More recently, Samson and Haddad[9] have measured the average charge produced per photon absorption from the threshold of double photoionization up to 107 eV.

While the electron-impact experiment yields the absolute oscillator strength of double photoionization, the direct photoabsorption measurements yield only the ratio of the cross sections for double and single photoionization. In Fig. 5, the results of the present calculation are given along with the experimental data of Carlson,[3] Van der Wiel and Wiebes,[7] and Samson and Haddad.[9] The photoionization yield is approximately given by

$$Y \approx \frac{\sigma^+ + 2\sigma^{++}}{\sigma^+ + \sigma^{++}} = \frac{1+2R}{1+R}, \tag{3.1}$$

where $R = \sigma^{++}/\sigma^+$ is the ratio of the cross sections for double (σ^{++}) and single (σ^+) photoionization. In

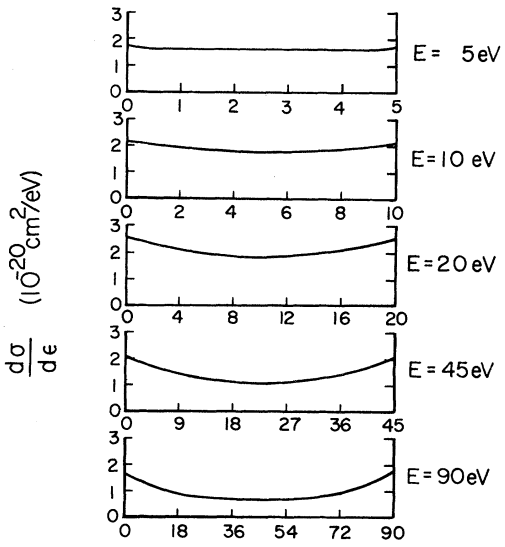

FIG. 4. Calculated photoelectron spectra for total kinetic energy $E = 5$, 10, 20, 45, and 90 eV.

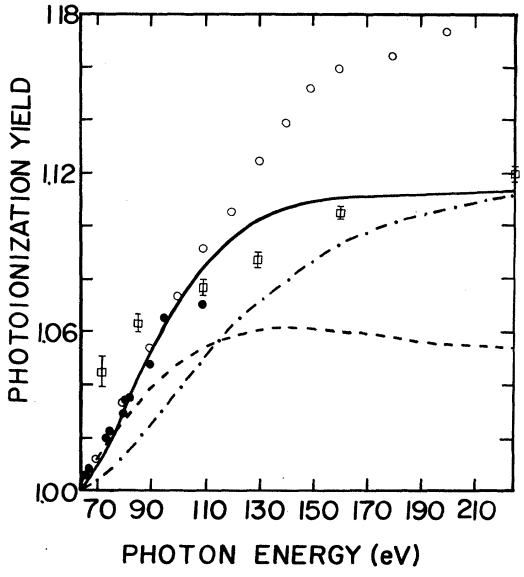

FIG. 5. Photoionization yield of neon as a function of photon energy. Present calculation, ————: total contribution [diagrams 1(a) +1(b) +1(c) +1(d) +1(e)], ----: diagram 1(a) alone, and -·-·-·-: diagrams 1(a) +1(b) +1(c); experimental measurement, ●: Samson and Haddad (Ref. 9), ○: Van der Wiel and Wiebes (Ref. 7), and □: Carlson (Ref. 3).

evaluating R, we have used the single photoionization oscillator strength shown in Fig. 6, which was calculated earlier in the dipole velocity approximation[19] using an MBPT approach similar to that of Kelly and Simons.[20]

Near threshold, our calculated result is in excellent agreement with the data of Samson and Haddad as well as with the result of the electron-impact experiment,[7] which should be reasonably reliable in this energy region where the momentum transfer is very small. [To some extent, this excellent agreement is accidental, since the photoionization yield depends also on the accuracy of the single photoionization cross sections which in our calculation agree with experiment to only about (5–10)%.] Carlson's data tend to be unduly high at this energy as a result of averaging over the wide band of his photon sources. On the other hand, this effect is less important at higher energy, and here both types of Carlson's data, from the charged-ion spectrometry and the photoelectron energy spectrum, are consistent and in agreement with our calculation. (It also agrees with the single measurement of Lightner *et al.*[6]) The large discrepancy between the data of Van der Wiel and Wiebes and that of Carlson is still not fully understood. While our calculation seems to be in better agreement with the data of Carlson, we should point out that we have neglected the contributions from (i) the final ionic configuration ($2s2p^5$), and (ii) the outgoing electrons in ($k_1 s\, k_2 p$) configurations.[21] Experimental measurements over the entire energy range of interest with a continuous light spectrum, such as that of synchrotron radiation, seem desirable.

D. Discussion

Examination of the analytic structure of the contributing terms points to several characteristic

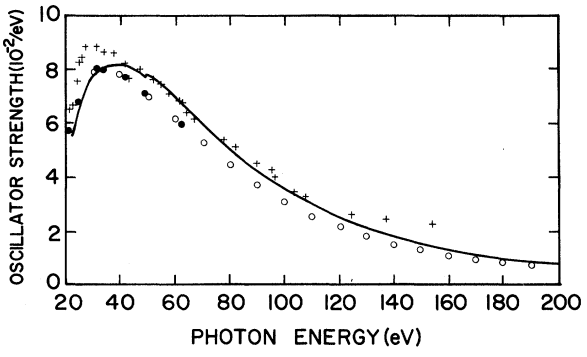

FIG. 6. Oscillator strength of neon single photoionization. Solid curve: MBPT velocity approximation (Ref. 19), ●: Samson (Ref. 25), +: Ederer and Tomboulian (Ref. 26), and ○: Van der Wiel and Wiebes (Ref. 7).

aspects of double photoionization. First, we find that at higher photon energies, the matrix elements $t_\alpha^f(k_1, k_2)$ of all important contributions, i.e., diagrams 1(a)–1(c), yield larger values when the energy of one of the outgoing electrons is much larger than that of the second electron. As an illustration, we examine the matrix element $t_\alpha^f(k_1, k_2)$ of diagram 1(a):

$$t_{1(a)}^f(k_1, k_2) = -\frac{\langle k_1 pnp|\, v\,|npnp\rangle\langle k_2 d|H_\gamma|np\rangle}{\frac{1}{2}k_1^2 + \Delta E},$$

where $\Delta E_{Ne^{++}} - E_{Ne} + \epsilon_{2p} = 3$ Ry. Note that the numerator varies very slowly as a function of k, since $\langle k_1 pnp|\, v\,|npnp\rangle$ and $\langle k_2 d|H_\gamma|np\rangle$ tend to compensate for each other,[22] while the energy denominator varies much faster as k_1^2 varies, indicating that $t_{1(a)}^f$ has larger values when k_1 is small and k_2 is large. Similar analytic considerations apply to diagrams 1(b) and 1(c). This effect becomes more prominent when we calculate the photoelectron energy spectrum which is obtained by taking the square of the sum of all three contributions. Therefore, at higher photon energies, most of the available kinetic energy is carried away by one of the outgoing electrons.

Second, we find that the effect of ground-state correlations remains significant even at high energies. As we just mentioned, most of the energy is carried away at higher energies by one of the outgoing electrons; therefore, the energy interval relevant to double photoionization is confined to a small part of the energy spectrum. For the core rearrangement [diagram 1(a)], this important energy region is restricted to that of smaller k_1, and the contribution of $\langle k_1 pnp|\, v\,|npnp\rangle/(\frac{1}{2}k_1^2 + \Delta E)$ in $t_{1(a)}^f$ to double photoionization is approximately independent of E_γ. In other words, the contribution from diagram 1(a) depends on the values of $\langle k_2 d|H_\gamma|np\rangle$ over a small range of k_2. Similarly, for the ground-state correlations diagram 1(b), contributions to double photoionization are restricted to a small portion of the energy spectrum. Their matrix elements $t_{1(b)}^f$ can be rewritten as

$$t_{1(b)}^f = \langle k_2 d|H_\gamma|\,\Phi_p\rangle,$$

where the state

$$|\,\Phi_p\rangle = \sum_{k_0} \frac{|k_0 p\rangle\langle k_0 p k_1 p|\, v\,|npnp\rangle}{2\epsilon_{np} - \epsilon_{k_1} - \epsilon_{k_0}}$$

has the character of a *bound p orbital*. Since both $\langle k_2 d|H_\gamma|np\rangle$ and $\langle k_2 d|H_\gamma|\,\Phi_p\rangle$ have the same k dependence at high energies, the relative importance of the ground-state correlations to the core rearrangement should remain fairly constant as energy increases. The importance of virtual Auger transition [diagram 1(c)] is determined by a matrix

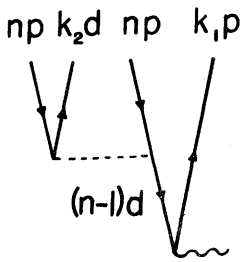

FIG. 7. Contributing term involving inner-shell electrons for double photoionization of heavier rare-gas atoms.

element $\langle k_1 p|H_\gamma|ns\rangle$. While its separate contribution is smaller than others, it decreases with increasing energy at a slightly slower rate than those of core rearrangement and ground-state correlations.

Third, the constant ratio of double to single photoionization at high energies, shown in Fig. 5, can also be understood through similar analysis. Note that the single photoionization is determined by the matrix element $\langle kd|H_\gamma|np\rangle$. At lower energies, k may be much larger than k_2 owing to different ionization thresholds of single and double photonionization; hence the ratio of $\langle k_2 d|H_\gamma|np\rangle$ to $\langle kd|H_\gamma|np\rangle$ may vary considerably. As E_γ increases, the ratio of double to single photoionization should reach an asymptotic value, since both $\langle k_2 d|H_\gamma|np\rangle$ and $\langle kd|H_\gamma|np\rangle$ have the same energy dependence.

The present study indicates that the major physical processes responsible for double photoionization of valence electrons of rare-gas atoms involve electrons from the same shell (ns and np electrons). However, increasing evidence suggests that inner-shell electrons also play an important part in the ionization of outer shells[23]; see particularly the recent calculation by Amusia[12] on Xe photoabsorption near 90 eV and the calculation of photoionization of the valence electron of Na and K by Chang.[24] Experimentally, a rapid rise in double photoionization below the triple-ionization threshold has been observed in Xe.[8,9] Figure 7 shows one of the possible contributions to this effect which involves inner-shell d electrons. This contribution should become significant when the photon energy approaches the ionization threshold of the $(n-1)d$ electrons. The observation by Samson and Haddad near the ionization threshold of the $4d$ electron seems to be consistent with this qualitative picture.

In conclusion, we are particularly encouraged by the qualitative understanding obtained in the present calculation. The good agreements between experiments and our numerical results further suggest that the present theoretical treatment has indeed provided a realistic approach for a systematic investigation of multiple photoionization. Further explorations along this direction are most desirable.

ACKNOWLEDGMENT

One of us (T.N.C.) would like to thank Professor U. Fano for his continued support and many valuable comments.

*Work supported in part by U. S. Energy Research and Development Administration, Contract No. COO-1674-105 at the University of Chicago and in part by the National Aeronautics and Space Adminstration, at the University of California at Riverside.

†Present address: Physics Department, University of Southern California, Los Angeles, California 90007.

[1]U. Fano and J. W. Cooper, Rev. Mod. Phys. 40, 441 (1968).

[2]T. Åberg, Ann. Acad. Sci. Fenn. A VI 308, 1 (1969); and in *Proceedings of the International Conference on Inner Shell Ionization Phenomena and Future Applications, Atlanta, Georgia, 1972,* edited by R. W. Fink, S. T. Manson, J. M. Palms, and P. V. Rao, CONF-720 404 (Natl. Tech. Information Service, U. S. Dept. of Commerce, Springfield, Va., 1972), p. 1509.

[3]T. A. Carlson, Phys. Rev. 156, 142 (1967).

[4]T. A. Carlson and M. O. Krause, Phys. Rev. 137, A1655 (1965); 140, A1057 (1965), 158, 18 (1967); M. O. Krause, T. A. Carlson, and R. D. Dismukes, Phys. Rev. 170, 37 (1968); F. Wuilleumier and M. O. Krause, Phys. Rev. A 10, 242 (1974).

[5]R. B. Cairns, H. Harrison, and R. I. Schoen, Phys. Rev. 183, 53 (1969).

[6]G. S. Lightner, R. J. Van Brunt, and W. D. Whitehead, Phys. Rev. A 4, 602 (1971).

[7]M. J. Van der Wiel and G. Wiebes, Physica 54, 411 (1971).

[8]M. J. Van der Wiel and G. Wiebes, Physica 53, 225 (1971); Th. M. El-Sherbini and M. J. Van der Wiel, Physica 62, 119 (1972).

[9]J. A. R. Samson and G. N. Haddad, Phys. Rev. Lett. 33, 875 (1974).

[10]F. W. Byron, Jr. and C. J. Joachain, Phys. Rev. 164, 1 (1967).

[11]T. N. Chang, T. Ishihara, and R. T. Poe, Phys. Rev. Lett. 27, 838 (1971).

[12]M. Ya. Amusia, *Atomic Physics 2,* edited by P. G. H. Sanders (Plenum, New York, 1971), p. 249; in *Proceedings of the Eighth International Conference on the Physics of Electronic and Atomic Collisions, Belgrade, 1973,* edited by B. C. Čobić and M. V. Kurepa (Institute of Physics, Belgrade, Yugoslavia, 1973), p. 171.

[13]H. P. Kelly, Adv. Chem. Phys. 14, 129 (1967); T. Ishi-

hara and R. T. Poe, Phys. Rev. A 6, 111 (1972); H. P. Kelly, Phys. Rev. A 6, 1048 (1972).
[14]J. Goldstone, Proc. R. Soc. Lond. A 239, 267 (1957); P. Nozieres, *Theory of Interacting Fermi Systems* (Benjamin, New York, 1964), Chap. 5.
[15]T. N. Chang and R. T. Poe, Phys. Rev. A 11, 191 (1975).
[16]S. Chandrasekhar, Astrophys. J. 102, 223 (1945); H. A. Bethe and E. E. Salpeter, *Quantum Mechanics of One- and Two-Electron Atoms* (Springer-Verlag, Berlin, 1957), p. 252.
[17]T. N. Chang and R. T. Poe, J. Comp. Phys. 12, 557 (1973).
[18]G. H. Wannier, Phys. Rev. 90, 817 (1953); A. R. P. Rau, Phys. Rev. A 4, 207 (1971); R. Peterkop, J. Phys. B 4, 513 (1971); S. Cvejanović and F. H. Read, J. Phys. B 7, 1841 (1974).
[19]T. N. Chang and R. T. Poe, Bull. Am. Phys. Soc. 17, 69 (1972).
[20]H. P. Kelly and R. L. Simons, Phys. Rev. Lett. 30, 529 (1973).
[21]Our calculation has shown that the contribution from the process with outgoing electrons in $(k_1 s, k_2 p)$ configuration is generally less than 5%, and the contribution from the process with the residual ion in $(2s2p^5)$ configuration is estimated to be less than 15% (Ref. 3).
[22]In the region of very small k_1, the matrix element $\langle k_1 pnp | v | npnp \rangle$ varies much faster. However, this is limited only to a very small energy region and does not affect our qualitative consideration.
[23]U. Fano, Comments At. Mol. Phys. 4, 119 (1973).
[24]T. N. Chang, J. Phys. B 8, 743 (1974).
[25]J. A. R. Samson, J. Opt. Soc. Am. 55, 935 (1965).
[26]D. L. Ederer and D. H. Tomboulian, Phys. Rev. 133, A1525 (1964).